8th Manufacturing Engineering Society International Conference

A comparative study of image processing thresholding algorithms on residual oxide scale detection in stainless steel production lines

Juan Miguel Cañero-Nieto[a,*], José Francisco Solano-Martos[a], Francisco Martín-Fernández[a]

[a]Department of Civil Engineering, Materials and Manufacturing, University of Málaga, Edificio de Ingenierías, Málaga 29071, Spain

Abstract

The present work is intended for residual oxide scale detection and classification through the application of image processing techniques. This is a defect that can remain in the surface of stainless steel coils after an incomplete pickling process in a production line. From a previous detailed study over reflectance of residual oxide defect, we present a comparative study of algorithms for image segmentation based on thresholding methods. In particular, two computational models based on multi-linear regression and neural networks will be proposed. A system based on conventional area camera with a special lighting was installed and fully integrated in an annealing and pickling line for model testing purposes. Finally, model approaches will be compared and evaluated their performance.

Keywords: Defect Detection; Image Processing; Machine Vision; Stainless Steel; Quality Inspection

1. Introduction

Since ever, product quality has been of interest on manufacturing processes. Current economic trends and globalization increase the competitiveness among worldwide manufacturers stimulating continuous improvement of quality as a high priority within production processes. For quality assurance, it is important analyze defects when they occur in the production line and eliminate or reduce them quickly into acceptable levels [1].

* Corresponding author. Tel.: +34-951-952-506 .
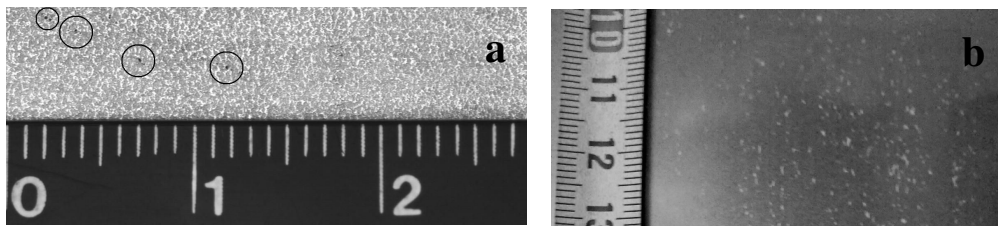 *E-mail address:* jmcanero@uma.es

Fig. 1. (a) Residual oxide scale; (b) Loss of quality effect on steel surface due to residual oxide scale after pickling and cold rolling.

Stainless steel is not a material outside the assurance of quality, rather, it is a product with high added value and importance today where the quality throughout the production process has a great impact on final costs. Initially melted and refined in a melting shop, stainless steel is rolled in a hot rolling mill at temperatures around 900ºC [2] and usually shaped as strip coil of several hundred meter length and different width and thickness. During this process, a layer composed mainly of ferrous and ferric oxides grows on the steel surface. This layer occurs as a result of the combustion of a certain oxygen concentration of non inert surrounding atmosphere with constituent elements from steel. The layer has to be removed in a subsequent pickling stage where coils undergo to a mechanical treatment with grain blasting and wire brush and also chemical treatment submerging them in acid tanks [3].

If this oxide layer is not completely removed from the steel surface, small oxide stains can remain attached randomly in the roughness of the surface (Fig. 1. (a)). When these stains measure less than tenth of a millimeter, they cannot be seen by the naked eye of the control quality staff on the line being undetectable. This failure of detection could produce several operational problems in succeeding production processes such as cold rolling process and, in the worst case scenario, the loss of quality of the steel surface lowering the value of material (Fig. 1. (b)).

Nowadays, machine vision is able to successfully solve defect detection and classification problems based on image processing algorithms with real-time requirements in industry. In this regard, different industrial approaches have been developed where some of them are clearly focused on surface defect detection and classification. To name a few: bearing inspection [4], defect detection of car body [5], wood defect classification [6], surface defects of film capacitors [7], classification of surface defects in friction stir welding [8], chemical imaging applied to product classification in pharmaceutical industry [9], quality inspection of injection molding process [10], quality assessment of additive manufacturing [11], defect detection of coated paper folding [12], surface defect detection of mobile phone screen [13], rail defect detection [14] and quality control in food industry [15].

In this paper, we present two computational models based on multi-linear regression and neural networks intended on image segmentation. The final goal will be the integration of models into a machine vision testing system installed in an annealing and pickling line for a residual oxide stains detection. The system will fulfill the time requirements of a real time application and also be adapted to the different steel grades and surface finishes.

2. Surface inspection systems

In general, a basic machine vision system for inspection is composed of one or more lighting devices, one or more cameras with optic lenses and computing hardware and software [16]. All of these elements are integrated into the factory for the acquisition and processing of camera images, acquisition of signals and/or data from factory, generation of results, decision making based on the analysis of results (which can be used to control other system or process), generation of alarms, display results or data storage of product that is being inspected. The image processing in machine vision systems can be classified mainly into five fundamental stages or steps to achieve the inspection requirements [17–19]: acquisition, pre-processing, segmentation, features extraction and classification.

Regarding image processing techniques for steel surface inspection, there is a large amount of literature showing the use of a wide variety of algorithms leading to the detection and classification of defects. These techniques can be categorized as statistical, morphological, spatial domain filtering, frequency domain analysis, joint spatial/frequency domain analysis and fractal models where morphological, spatial domain filtering and joint spatial/frequency domain analysis techniques are mostly used for all types of steel surfaces [20].
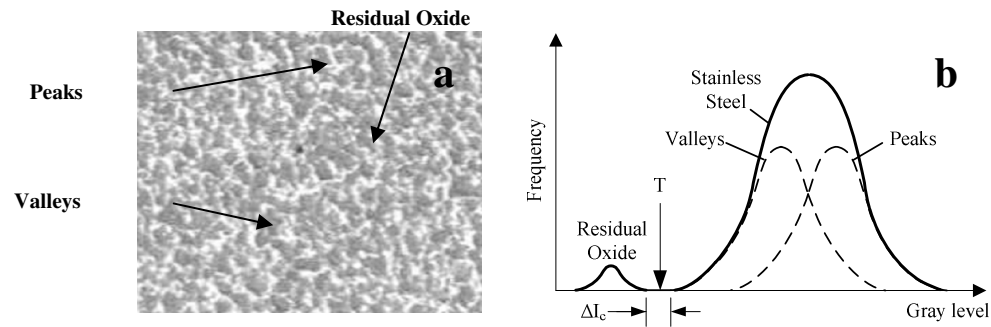
Fig. 2. (a) Stainless steel surface image with residual oxide stain; (b) Ideal histogram from image.

3. Oxide scale characterization

This section summarizes experimental results obtained after testing several stainless steel samples with and without residual oxide scale to reflectance tests. The samples were chosen from different steel grades and finishes. The final goal of these tests is the search for wavelength ranges of spectrum where the contrast between stainless steel surface with and without residual oxide scale defect is maximized.

The sample tests were carried out by the Industrial Automatic Institute from Spanish National Research Council (CSIC) in Madrid (Spain). A summary of this study can be found in [21].

The spectral curves were obtained for a wavelength range between 200 a 2400 nm covering NUV (Near-Ultra Violet), VIS (Visible) and NIR (Near-Infrared) electromagnetic bands. After analyzing spectral curves, it can be concluded that the best conditions to discriminate stainless steel from residual oxide stains are obtained within VIS band.

When clean stainless steel surface images are acquired by a VIS camera, the image average luminance obtained depends on the reflectance obtained from the inspected surface and this, in turns, basically on steel grade and surface roughness.

The hypothesis is that if there is any residual oxide stain in an image (Fig. 2. (a)), its reflectance will be lower than reflectance of the valleys of the roughness. This can be seen in an ideal histogram of the image where the grey levels of residual oxide stain are lower than the stainless steel grey level (Fig. 2. (b)).

The success in defect detection will depend on the ability to separate the residual oxide stains from clean stainless steel and therefore on the existing level of contrast ΔI_c. In a real situation, the contrast between them will not be so obvious, hence the difficulty to perform the defect detection. This difficulty can be originated mainly by the following causes: (1) existing noise in the image which introduces gray levels between two main lobes (defect and steel surface); (2) uneven lighting on surface; (3) internal reflections originated by surface roughness; (4) Existence of other defects on surface.

Finally, the goal of the defect detection algorithm will be to obtain the best threshold value *T* in an image histogram to discriminate effectively defects from steel surface.

4. Segmentation by thresholding techniques

Segmentation techniques based on thresholding are relatively simple and attractive due to their low computational cost. Its application is very interesting when there is contrast between pixel gray levels belonging to an object to be segmented and those belonging to background of the image. The thresholding result of quantized image in gray levels f(x,y) is a binary image g(x,y) in which each image position (x,y) may belong to a state or its complementary (e.g., background and foreground). The separation between them it is done based on the intensity levels existing in the image and the value of certain threshold function *T* where p(x,y) can be a local property in the neighborhood of point (x,y). Therefore, the thresholded image can be defined as [19]:

$$g(x,y) \begin{cases} =1 & f(x,y){\geq}T \\ =0 & f(x,y){<}T \end{cases} \tag{1}$$

Thresholding algorithms can be categorized according to the type of information that they use to find the best threshold T. These categories are the following [22]: (1) *Histogram shape-based methods* (analysis of the histogram shape to select the threshold); (2) *Clustering-based methods* (grouping of image gray levels into background and foreground); (3) *Entropy-based methods* (use of the entropy of pixel gray level distribution to discriminate between background and foreground); (4) *Object attributes-based methods*(use of attribute quality or similarity measures between original and binarized images; (5) *Spatial methods* (analysis of probability distributions and correlations between pixels); (5) *Local adaptive methods* (threshold calculation for each pixel based on some local statistics).

5. Mathematical models

The linear regression analysis is a statistical technique used to explore and quantify the relationship between a dependent variable Y and one or more variables called independents $(X_1, X_1, \cdots, X_k)$, as well as, to develop a mathematical model for predictive purposes. In a multiple regression analysis, the regression equation no longer defines a line in a plane but a hyperplane in a multidimensional space. The equation of the multiple regression model is defined as [23]:

$$Y = \beta_0 + \beta_1 \cdot X_1 + \beta_2 \cdot X_2 + \cdots + \beta_k \cdot X_k + \epsilon \tag{2}$$

where k is the number of independent variables in equation, β_0 is a constant, β_i $(i = 1, 2, \cdots, k)$ is the relative weight for independent variable X_i and ϵ is the residual term of the model. The statistical model is based on several assumptions or conditions which must be fulfilled for model validation: linearity, independence, normality, homoscedasticity and non-collinearity.

Neural networks are computational models based on a parallel-distributed architecture with learning ability by means of examples. This learned knowledge is stored in the form of neuron connections weighted by a specific weight [24,25]. The multilayer perceptron networks (MLP) is one of the most well-known neural networks [26]. It is a feed-forward network where input and output spaces are statically mapped. The MPL is built of multiple layers of neurons which can be used to solve not linearly separable problems and also as an universal estimation method. The function Y_i for one hidden layer MPL is the following:

$$Y_i = g_1 \cdot \sum_{j=1}^{M} [w_{ij} \cdot s_j] = g_1 \cdot \sum_{j=1}^{M} \left[w_{ij} \cdot \left(g_2 \cdot \sum_{r=1}^{L} [t_{jr} \cdot x_r] \right) \right] \tag{3}$$

where L is the neuron number in hidden layer, M the neuron number in output layer, g_1 the transfer function of output layer units, g_2 is the transfer function of hidden layer units and t_{rj} synaptic weight between hidden layer neuron j and input layer neuron r.

6. Machine vision system for testing algorithms

The machine vision system for testing has been installed in an annealing and pickling line at factory (Fig. 3). It consists of a high resolution camera, stroboscopic light and diffusing screens, all of them inside a hermetic steel case placed in a slide which can be displaced transversally to the sheet movement [27]. This system continually sample the surface, moving the acquisition device across the coil width and taken several images per second. The images acquired are in gray scale, 32 x 27 mm size and 1270 x 870 pixels resolution. These values have been selected to guarantee that a 50 μm stain will contain enough pixels to be detected. The acquired images are sent to an industrial embedded computer which will process the images to obtain the inspection results. This processing computer is connected to the factory LAN so that the processing results are presented in real time to the quality control operators and the images acquired and processed can be reviewed and even stored for back office supervision.
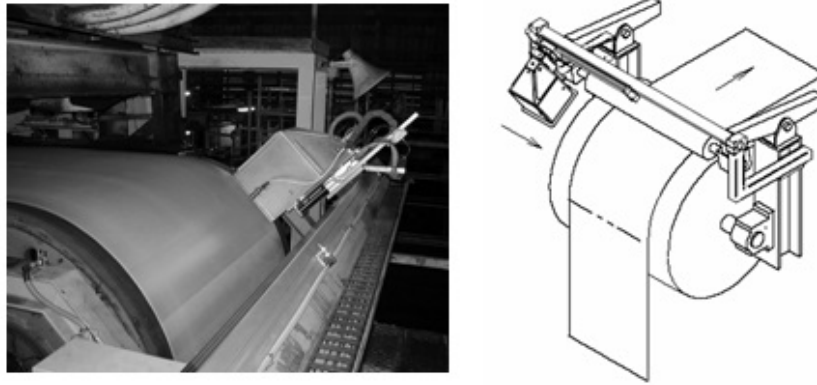
Fig. 3. Machine vision system working on site.

7. Image processing algorithm

The image processing task must solve the strategy to perform a reliable and robust residual oxide detection and classification from the images acquired by the camera. This strategy will be based on a new segmentation technique where defect discrimination will be performed analyzing the histogram shape of image and integrating empirical knowledge acquired previously.

During the image preprocessing stage a series of operations will be carried out on the image to adapt it to subsequent stage of segmentation. They are the followings:

- High frequency noise removing/reduction in the image and contrast enhancement between the residual oxide stains and the defect-free surface. This operation will be carried out by filtering with preserved edges.
- Obtaining the histogram from the filtered image.
- Smoothing the histogram by applying a FIR (finite impulse response) filter.

The goal of the segmentation stage will be to find a threshold T in the smoothed histogram that discriminates those pixels considered as a defect of those that correspond to defect-free surface. Not all processed images will contain defects and, in these, the threshold founded must assign all the pixels to the class that considers the surface free of defect. The basic sequence to be performed for the segmentation of an image will be composed of the following operations (Fig. 4. (a)):

- From an empirical mathematical model, obtain a threshold T_e^* which will determine a gray level range where the search of the binarization threshold T will be performed. The model inputs are composed of an input vector with features extracted from the image histogram.
- Determination of gray level dynamic range $[n_{min}, n_{max}]$ for searching threshold T.
- Search of the threshold T in the smoothed histogram of image within the dynamic range. This search will try to find the deepest minimum in the dynamic range defined (Fig. 4. (b)).
- Image binarization from the threshold T found.

The final purpose of the image acquisition and processing is to give a measurement of the amount and grade of the residual scale detected, as well as, a classification of stains by grouping them in several classes according to their dimension (50-100, 100-150, 150-200 and more than 200 μm).
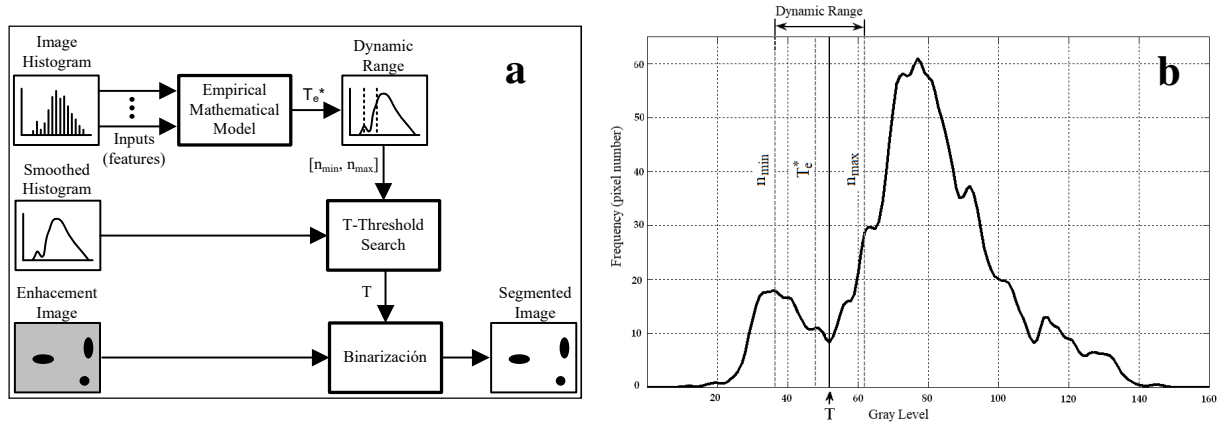
Fig. 4. (a) Segmentation stage workflow and (b) searching deepest minimum in dynamic range to find threshold *T*.

8. Empirical mathematical models

An empirical mathematical model is needed to obtain a threshold T_e^* which determines a gray level range for searching the binarization threshold *T*. A heuristic methodology based on the use of expert knowledge in residual oxide detection will be applied for model construction.

The images taken by the camera which contain residual oxide defects will be presented to the human expert for the knowledge acquisition task. The human expert has to identify residual oxide stains within the image and determine the best threshold that discriminates the residual oxide stains on stainless steel surface.

The set of images shown to the expert belong to a wide variety of austenitic and ferritic steel grades with different surface finishes (ASTM 301, 304 304L, 304, 309 S, 310S, 316, 316L, 316 Ti, 321, 409L, 430, 430 Ti, 430 Nb, 434). This set forms a representative number of all types of stainless steel that are processed in the annealing and pickling line.

After that, statistical information will be extracted in the form of indexes from the gray-level histogram of each image: standard deviation, kurtosis, skewness and median from image. These indexes will be part of the input vector during the model construction.

The mathematical model input vector choice has not been made randomly but based on a series of characteristics observed after analyzing the histogram shapes from the images:

- Steel surfaces, where the valleys predominate over the peaks, present histograms biased to the left and, on the contrary, if the peaks predominate over the valleys they are biased to the right.
- Surfaces with large differences in height between valleys and peaks have more gray levels obtaining greater values of standard deviation and kurtosis (platykurtic behavior), and on the contrary, small height differences obtaining smaller values of standard deviation and kurtosis (leptokurtic behavior).
- The steel grades and surface finishes originate image histograms where median values are displaced along the gray level axis.

Once the acquisition of knowledge is completed, the mathematical model will be made. This model will be evaluated using cross-validation method where the total population (1774 images) is separated in groups of 80%, 10% and 10% for the model training, validating and testing, respectively.

The model construction is carried out through two types of techniques: multi-linear regression and neural networks. Both empirical mathematical models will predict the value of the threshold T_e^*. This value will be the dependent variable in linear model and the neural network output in neural network model. The tools used for the construction of the models were IBM SPSS 22 for linear model and Matlab Neural Network Toolbox 8.3 for neural model. Table 1 shows the multi-linear regression model independent variables and coefficients (non standardized β_i and standardized BETA) obtained after performing the regression and validation of the model.

The optimal neural network model was a MLP with one hidden layer with five neurons and one neuron in the output layer. The transfer function selected was the hyperbolic tangent for the hidden layer and the linear function for the output layer. The network training was performed based on Levenberg-Marquardt algorithm.

The models have been analyzed and compared between them from simple and intuitive statistical indexes such as the mean absolute error (AE_{mean}), maximum absolute error (AE_{max}) and absolute error standard deviation (σ_{AEmean}). They are obtained based on the absolute error AE calculated for each sample image of the population, shown in equation (4), where T_e is the optimal threshold selected by human expert.

$$AE = |T_e - T_e^*| \tag{4}$$

The comparison of both models is shown in Table 2 where it can be seen a better performance of the neural network model with lower values of AE_{mean}, AE_{max} and σ_{AEmean}.

Table 1. Multiple linear regression model coefficients.

k	X_k Input Variable	β_k	BETA
0	-	10.144	-
1	Median	0.801	0.966
2	Standard Dev.	-0.956	-0.259
3	Kurtosis	-1.041	-0.172
4	Skewness	1.347	0.084

Table 2. Error statistical indexes model comparison.

Model	AE_{mean}	AE_{max}	σ_{AEmean}
Multiple Linear	2.07	12.99	1.63
Neural Network	1.92	6.76	1.47

Once the empirical model has been chosen, the gray level dynamic range $[n_{min}, n_{max}]$ can be set from error statistical indexes and threshold T_e^* as shown in equation (5).

$$[n_{min}, n_{max}] = [T_e^* - (AE_{mean} + 3 \cdot \sigma_{AEmean}), \ T_e^* + (AE_{mean} + 3 \cdot \sigma_{AEmean})] \tag{5}$$

9. Conclusions

In this paper, two new image processing algorithms have been presented, tested and compared to detect and classify the rate and size of residual oxide stains in a stainless steel production line. The image processing strategy for detecting and classifying defects integrates new segmentation methods based on the integration of empirical knowledge for an automatic histogram thresholding based on the histogram shape contributing to the improvement of quality in the process. This strategy has the following characteristics:

- Detect residual oxide on stainless steel surfaces in movement of a reliable, robust and efficient manner taking into account the variety of steel grades and surface finishes. It quantify the residual oxide detected on the surface and classify it into groups dimensions defined by the manufacturer.
- Two empirical mathematical models based on a linear regression and neural network have been proposed to obtain the search range for binarization threshold. Descriptive data were extracted from a population of previously characterized images by an expert. The two models have been compared, finding a better behavior in the neuronal model.

References

[1] S. Kalpakjian, S.R. Schmid, Manufacturing, Engineering and Technology, 5th ed., Pearson Education, 2008.
[2] B.K. Jha, P. Jha, C.D. Singh, Process technology for the continuous hot band annealing of 17%Cr ferritic stainless steel, J. Mater. Eng.

Perform. 11 (2002) 180–186. doi:10.1361/105994902770344240.

[3]   P. Shi, H. Shi, C. Liu, M. Jiang, Effect of pickling process on removal of oxide layer on the surface of ferritic stainless steel, Can. Metall. Q. 57 (2018) 168–175. doi:10.1080/00084433.2017.1405540.

[4]   H. Shen, S. Li, D. Gu, H. Chang, Bearing defect inspection based on machine vision, Meas. J. Int. Meas. Confed. 45 (2012) 719–733. doi:10.1016/j.measurement.2011.12.018.

[5]   J. Molina, J.E. Solanes, L. Arnal, J. Tornero, On the detection of defects on specular car body surfaces, Robot. Comput. Integr. Manuf. 48 (2017) 263–278. doi:10.1016/j.rcim.2017.04.009.

[6]   K. Kamal, R. Qayyum, S. Mathavan, T. Zafar, Wood defects classification using laws texture energy measures and supervised learning approach, Adv. Eng. Informatics. 34 (2017) 125–135. doi:10.1016/j.aei.2017.09.007.

[7]   Y. Yang, Z.J. Zha, M. Gao, Z. He, A robust vision inspection system for detecting surface defects of film capacitors, Signal Processing. 124 (2016) 54–62. doi:10.1016/j.sigpro.2015.10.028.

[8]   R. Ranjan, A.R. Khan, C. Parikh, R. Jain, R.P. Mahto, S. Pal, S.K. Pal, D. Chakravarty, Classification and identification of surface defects in friction stir welding: An image processing approach, J. Manuf. Process. 22 (2016) 237–253. doi:10.1016/j.jmapro.2016.03.009.

[9]   C. Gendrin, Y. Roggo, C. Collet, Pharmaceutical applications of vibrational chemical imaging and chemometrics: A review, J. Pharm. Biomed. Anal. 48 (2008) 533–553. doi:10.1016/j.jpba.2008.08.014.

[10]   Y. Yang, B. Yang, S. Zhu, X. Chen, Online quality optimization of the injection molding process via digital image processing and model-free optimization, J. Mater. Process. Technol. 226 (2015) 85–98. doi:10.1016/j.jmatprotec.2015.07.001.

[11]   K. Rane, K. Castelli, M. Strano, Rapid surface quality assessment of green 3D printed metal-binder parts, J. Manuf. Process. 38 (2019) 290–297. doi:10.1016/j.jmapro.2019.01.032.

[12]   M. Pál, D. Novaković, S. Dedijer, L. Koltai, I. Jurič, G. Vladić, N. Kašiković, Image processing based quality control of coated paper folding, Meas. J. Int. Meas. Confed. 100 (2017) 99–109. doi:10.1016/j.measurement.2016.12.033.

[13]   C. Jian, J. Gao, Y. Ao, Automatic surface defect detection for mobile phone screen glass based on machine vision, Appl. Soft Comput. J. 52 (2017) 348–358. doi:10.1016/j.asoc.2016.10.030.

[14]   S. Hajizadeh, A. Núñez, D.M.J. Tax, Semi-supervised Rail Defect Detection from Imbalanced Image Data, IFAC-PapersOnLine. 49 (2016) 78–83. doi:10.1016/j.ifacol.2016.07.014.

[15]   M. Shamili, The estimation of mango fruit total soluble solids using image processing technique, Sci. Hortic. (Amsterdam). 249 (2019) 383–389. doi:10.1016/j.scienta.2019.02.013.

[16]   B.G. Batchelor, P.F. Whelan, Intelligent Vision Systems for Industry, Springer-Verlag Berlin Heidelberg, 2002. doi:10.1007/s12237-010-9326-x.

[17]   B. Jähne, Digital Image Processing, Sixth, Springer-Verlag, Berlin, Heidelberg, Germany, 2005.

[18]   W.K. Pratt, Digital Image Processing, Fourth, Wiley-Interscience, Hoboken, New Jersey, U.S.A., 2007.

[19]   R.C. Gonzalez, R.E. Woods, Digital Image Processing, Second, Prentice Hall, Upper Saddle River, New Jersey 07458, U.S.A., 2002. doi:10.1111/j.1365-313X.2011.04896.x.

[20]   N. Neogi, D.K. Mohanta, P.K. Dutta, Review of vision-based steel surface inspection systems, J. Image Video Process. 2014 (2014). doi:10.1186/1687-5281-2014-50.

[21]   D. Martin, D. Guinea, E. Garcia-Alegre, D.M. Guinea, Multi-modal defect detection of residual oxide scale on a cold stainless steel strip, in: Mach. Vis. Appl., 2010: pp. 653–666. doi:10.1007/s00138-010-0260-5.

[22]   M. Sezgin, B. Sankur, Survey over image thresholding techniques and quantitative performance evaluation, 13 (2004) 146–165. doi:10.1117/1.1631316.

[23]   A.M. Mathai, H.J. Haubold, Probability and Statistics. A Course for Physicist and Engineers, De Gruyter, Berlin, Germany, 2018.

[24]   M. Minsky, S.A. Papert, Perceptrons: An Introduction to Computational Geometry, MIT Press, Cambridge, MA, U.S.A., 1969.

[25]   F. Rosenblatt, The Perceptron: a Probabilistic Model for Information Storage and Organization in the Brain, Psychol. Rev. 65 (1958) 386–408.

[26]   D.W. Patterson, Artificial Neural Networks: Theory and Applications, 1st., Prentice Hall, New Jersey, NY, U.S.A., 1998.

[27]   C. Gonzalez Spínola, F. García Vacas, M.J. Martín Vázquez, J. Vizoso Laporte, S. Espejo Meana, J.M. Cañero Nieto, S. Morillas Castillo, D. Guinea Diaz, E. Villanueva Martinez, D. Martín Gómez, J.M. Bonelo Sánchez, Device for Detecting and Classifying Residual Oxide in Metal Sheet Production Lines, 2008/119845, 2008.